Sex differences in the structural connectome of the human brain

Madhura Ingalhalikar[a,1], Alex Smith[a,1], Drew Parker[a], Theodore D. Satterthwaite[b], Mark A. Elliott[c], Kosha Ruparel[b], Hakon Hakonarson[d], Raquel E. Gur[b], Ruben C. Gur[b], and Ragini Verma[a,2]

[a]Section of Biomedical Image Analysis and [c]Center for Magnetic Resonance and Optical Imaging, Department of Radiology, and [b]Department of Neuropsychiatry, Perelman School of Medicine, University of Pennsylvania, Philadelphia, PA 19104; and [d]Center for Applied Genomics, Children's Hospital of Philadelphia, Philadelphia, PA 19104

Sex differences in human behavior show adaptive complementarity: Males have better motor and spatial abilities, whereas females have superior memory and social cognition skills. Studies also show sex differences in human brains but do not explain this complementarity. In this work, we modeled the structural connectome using diffusion tensor imaging in a sample of 949 youths (aged 8–22 y, 428 males and 521 females) and discovered unique sex differences in brain connectivity during the course of development. Connection-wise statistical analysis, as well as analysis of regional and global network measures, presented a comprehensive description of network characteristics. In all supratentorial regions, males had greater within-hemispheric connectivity, as well as enhanced modularity and transitivity, whereas between-hemispheric connectivity and cross-module participation predominated in females. However, this effect was reversed in the cerebellar connections. Analysis of these changes developmentally demonstrated differences in trajectory between males and females mainly in adolescence and in adulthood. Overall, the results suggest that male brains are structured to facilitate connectivity between perception and coordinated action, whereas female brains are designed to facilitate communication between analytical and intuitive processing modes.

diffusion imaging | gender differences

Sex differences are of enduring scientific and societal interest because of their prominence in the behavior of humans and nonhuman species (1). Behavioral differences may stem from complementary roles in procreation and social structure; examples include enhanced motor and spatial skills and greater proclivity for physical aggression in males and enhanced verbally mediated memory and social cognition in females (2, 3). With the advent of neuroimaging, multiple studies have found sex differences in the brain (4) that could underlie the behavioral differences. Males have larger crania, proportionate to their larger body size, and a higher percentage of white matter (WM), which contains myelinated axonal fibers, and cerebrospinal fluid (5), whereas women demonstrate a higher percentage of gray matter after correcting for intracranial volume effect (6). Sex differences in the relative size and shape of specific brain structures have also been reported (7), including the hippocampus, amygdala (8, 9), and corpus callosum (CC) (10). Furthermore, developmental differences in tissue growth suggest that there is an anatomical sex difference during maturation (11, 12), although links to observed behavioral differences have not been established.

Recent studies have used diffusion tensor imaging (DTI) to characterize WM architecture and underlying fiber tracts by exploiting the anisotropic water diffusion in WM (13–15). Examination of DTI-based scalar measures (16) of fractional anisotropy (FA) and mean diffusivity (MD) has demonstrated diverse outcomes that include increased FA and decreased MD in males in major WM regions (17–19), higher CC-specific FA in females (20, 21), and lower axial and radial diffusivity measures (22) in males. Throughout the developmental period, females displayed higher FA and lower MD in the midadolescent age

(12–14 y) (23), and this result was established on a larger sample size (114 subjects) as well (24). On the other hand, sex differences on the entire age range (childhood to old age) demonstrated higher FA and lower MD in males (19, 25, 26). Similar findings of higher FA in males were obtained with tractography on major WM tracts (27, 28).

Rather than investigating individual regions or tracts in isolation, the brain can be analyzed on the whole as a large and complex network known as the human connectome (29). This connectome has the capability to provide fundamental insights into the organization and integration of brain networks (30). Advances in fiber tractography with diffusion imaging can be used to understand complex interactions among brain regions and to compute a structural connectome (SC) (31). Similar functional connectomes (FCs) can be computed using modalities like functional MRI, magnetoencephalography, and EEG. Differences in FCs have revealed sex differences and sex-by-hemispheric interactions (32), with higher local functional connectivity in females than in males (33). Although SCs of genders have displayed small-world architecture with broad-scale characteristics (34, 35), sex differences in network efficiency have been reported (36), with women having greater overall cortical connectivity (37). Insignificant differences between the genders were observed in a recent study on SCs of 439 subjects ranging in age from 12–30 y (38). However, detailed analysis on a very large sample is needed to elucidate sex differences in networks reliably, as is provided in this study. Using connection-wise regional and

Significance

Sex differences are of high scientific and societal interest because of their prominence in behavior of humans and non-human species. This work is highly significant because it studies a very large population of 949 youths (8–22 y, 428 males and 521 females) using the diffusion-based structural connectome of the brain, identifying novel sex differences. The results establish that male brains are optimized for intrahemispheric and female brains for interhemispheric communication. The developmental trajectories of males and females separate at a young age, demonstrating wide differences during adolescence and adulthood. The observations suggest that male brains are structured to facilitate connectivity between perception and coordinated action, whereas female brains are designed to facilitate communication between analytical and intuitive processing modes.

lobar analyses of DTI-based SCs of 949 healthy young individuals, we present a comprehensive study of developmental sex differences in brain connectivity.

Results

We present results from a cohort of 949 healthy subjects aged 8–22 y (mean ± SD = 15.11 ± 3.50 y), including 428 males (mean ± SD = 14.94 ± 3.54 y) and 521 females (mean ± SD = 15.25 ± 3.47 y) (demographic details are provided in Table 1). The DTI for creating SCs was performed at a b value of 1,000 s/mm^2 with 64 gradient directions on a Siemens 3T Verio scanner. Creating the SCs involved parcellating the brain into 95 regions (68 cortical and 27 subcortical) using a high-resolution T1 image, followed by interregional probabilistic fiber tractography, which provides the connection probability between regions, leading to the construction of the 95 × 95 network matrix called the SC of the brain (schematic in Fig. 1). Connection-wise analysis of these SC network matrices, followed by an examination of network properties using global, lobar, and regional measures, was performed. Because the age range in this population is large, to examine developmental sex differences, the population was divided into three groups, such that they have balanced sample sizes: group 1 (8–13.3 y, 158 females and 156 males), group 2 (13.4–17 y, 180 females and 131 males), and group 3 (17.1–22 y, 183 females and 141 males). These groups correspond roughly to the developmental stages of childhood, adolescence, and young adulthood. Connection-wise and global analyses were performed in each group. Details are given in *Materials and Methods*.

Connection-Wise Analysis. Linear regression was applied to each of the connections in the SC matrix on sex, age, and age–sex interaction. Permutation testing (20,000 permutations over all the edges in the network taken together) was used to address the problem of multiple comparisons in the connection-based network analysis. This analysis revealed conspicuous and significant sex differences that suggest fundamentally different connectivity patterns in males and females (Fig. 2). Most supratentorial connections that were stronger in males than females were intrahemispheric (permutation-tested $P < 0.05$). In contrast, most supratentorial connections that were stronger in females were interhemispheric. However, in the cerebellum, the opposite pattern prevailed, with males showing stronger connections between the left cerebellar hemisphere and the contralateral cortex.

Developmental differences were studied based on the three groups described above. Connection-based analysis revealed a progression of sex differences. The youngest group (aged 8–13.3 y) demonstrated a few increased intrahemispheric connections in

males and increased interhemispheric connections in females, suggesting the beginning of a divergence in developmental trajectory (Fig. 2B). This was supported by the results from the adolescent group (aged 13.4–17 y), as well as from the young adult group, where sex differences were more pronounced, with increased interhemispheric and intrahemispheric connectivity in females and males, respectively. However, in the adolescent group, the significant interhemispheric connections displayed by the females were concentrated in the frontal lobe, whereas during adulthood, females showed fewer significant edges that were dispersed across all the lobes.

Hemispheric and Lobar Connectivity. The connection-wise analysis of the SCs can be quantified at the lobar level by the hemispheric connectivity ratio (*HCR*). The *HCR* is computed for each lobe and quantifies the dominance of intra- or interhemispheric connections in the network matrices, with a higher lobar *HCR* indicating an increased connection of that lobe within the hemisphere. We found significantly higher *HCR*s in males in the left frontal ($P < 0.0001$, $T = 4.85$), right frontal ($P < 0.0001$, $T = 5.33$), left temporal ($P < 0.0001$, $T = 4.56$), right temporal ($P < 0.0001$, $T = 4.63$), left parietal ($P < 0.0001$, $T = 4.31$), and right parietal ($P < 0.0001$, $T = 4.59$) lobes, indicating that males had stronger intrahemispheric connections bilaterally.

We also computed the magnitude of connectivity using the lobar connectivity weight (*LCW*). The *LCW* quantifies the connection weight between any two lobes. Consistent with the network differences observed in Fig. 2A and the *HCR* results, interlobar *LCW* in the same hemisphere was stronger in males, whereas left-to-right frontal lobe connectivity was higher in females (Table 2).

High Modularity and Transitivity in Males. Of the several indices of network integrity (39), two measures of segregation, modularity and transitivity, are particularly well suited for describing differences in network organization. Modularity describes how well a complex neural system can be delineated into coherent building blocks (subnetworks). Transitivity characterizes the connectivity of a given region to its neighbors. Higher transitivity indicates a greater tendency for nodes to form numerous strongly connected communities. Both modularity and transitivity were globally higher in males (T statistic = 6.1 and 5.9, $P < 0.0001$, respectively), consistent with stronger intrahemispheric connectivity. Global transitivity was higher in males among all three groups (children: $T = 3.1$, $P = 0.003$; adolescents: $T = 4.9$, $P < 0.0001$; young adults: $T = 3.7$, $P = 0.0003$), whereas global modularity was significantly higher in adolescents and young adult males ($T = 5.1$, $P < 0.0001$ and $T = 2.7$, $P = 0.005$, respectively). Transitivity was also computed at the lobar level for the entire population to quantify the density of the clustered brain networks in each lobe. Local transitivity was higher in males [significant in frontal lobe, $T = $ (left) 3.97, (right) 4.13; significant in temporal lobe, $T = $ (left) 4.96, (right) 4.09; all $P < 0.0001$] suggesting stronger intralobar connectivity.

Differences in Participation Coefficients. Finally, we examined the participation coefficient (*PC*) of each individual regional node of the SC. The *PC* is close to one if its connections are uniformly distributed among all the lobes, and it is zero if all links connect within its own lobe. We found that numerous regions in the frontal, parietal, and temporal lobes had significantly higher *PC*s in females than in males (Fig. 3 and Table 3), whereas the cerebellum was the only region that displayed higher *PC*s in males.

Discussion

The study examined sex differences in a large population of 949 youths by comprehensively analyzing the diffusion-based SCs of the brain. Because the population has a large age range (8–22 y), we also examined the sex differences during the course of development. Our analysis resulted in several findings, some confirming earlier hypotheses and some providing unique insight

Table 1. Subject demographics

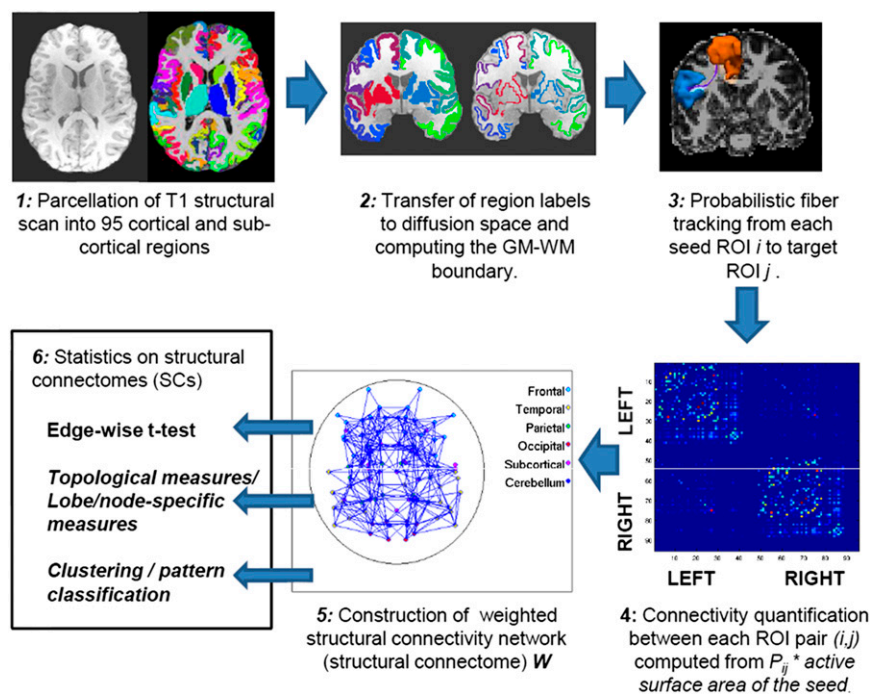| Race	Male		Female		Total	
Caucasian, not Hispanic	212	22.3%	206	21.7%	418	44.0%
Caucasian, Hispanic	8	0.8%	6	0.6%	14	1.5%
African American, not Hispanic	150	15.8%	234	24.7%	384	40.5%
African American, Hispanic	2	0.2%	7	0.7%	9	0.9%
Asian, not Hispanic	1	0.1%	9	0.9%	10	1.0%
Mixed/other, not Hispanic	37	3.9%	35	3.7%	72	7.6%
Mixed/other, Hispanic	18	1.9%	24	2.5%	42	4.4%
Total	428	45.1%	521	54.9%	949	100.0%
Mean age, y (SD)	14.9	(3.5)	15.3	(3.5)	15.1	(3.5)

Fig. 1. Schematic of the pipeline for creating the SC.

into sex differences that were not possible with alternate modalities and forms of analysis.

The myelinated axons of WM facilitate distant signal conduction. Previous data from structural imaging showed a higher proportion of cortical WM in the males, except in the CC (40, 41). A higher proportion of myelinated fibers within hemispheres in males compared with an equal or larger volume of WM in the callosum suggests that male brains are optimized for communicating within the hemispheres, whereas female brains are optimized for interhemispheric communication. Our analysis overwhelmingly supported this hypothesis at every level (global, lobar, and regional) and also revealed unique sex and developmental differences in the SC. Centered on connection-based analysis, we established that male brains are indeed structured to facilitate intrahemispheric cortical connectivity, although the opposite was observed in the cerebellum (Fig. 2A). In contrast, female brains displayed higher interhemispheric connectivity. The results of connection-based analysis are supported by the values of the *HCR* and *LCW* computed for the connectomes. Males had a higher *HCR* in the frontal, temporal, and parietal lobes bilaterally, indicating a higher connection within the hemisphere and within lobes. The *LCW* quantifies the relationship between lobes, with the males having higher within-hemisphere and across-lobe connections. In females, both of the values indicated across-hemisphere lobar connections.

With the aim of identifying at what stage of development these sex differences manifest themselves, we analyzed the population in three groups that align with childhood, adolescence, and young adulthood. The connectivity profiles showed an early separation (Fig. 2B) between the developmental trajectories of the two genders, with adolescent (Fig. 2C) and young adult (Fig. 2D) males displaying higher intrahemispheric connectivity and females of the same age displaying higher interhemispheric connectivity. Although the dominance of intrahemispheric connectivity in males was established early on and preserved throughout the course of development, interhemispheric connectivity dominance in females was seen mainly in the frontal lobe during adolescence but was more dispersed across the lobes during adulthood. Also, the gradual decrease of the dominance of interhemispheric connectivity in adulthood is most likely due to the fact that the inter-

hemispheric connections are of lower strength than the intra-hemispheric connections. The lack of a significant age-by-sex interaction in the connection-based analysis suggests that although there are not statistically significant differences in the trajectory of developmental effects between males and females, analyses of age groups allows the description of the magnitude of the sex difference during the stages of development.

In addition to the connection-wise analysis, we investigated two complementary network measures, modularity and transitivity, at the global level and found these to be higher in males than in females. These measures quantify the sparsity of the connectome, that is, how easily it can be divided into subnetworks. A high lobar-level transitivity points to a region's neighbors being more strongly connected to each other within each lobe. A higher lobar transitivity showed that local clustering into subnetworks was high in males, resulting in an increased global modularity. This is indicative again of the enhanced local, short range within lobe connectivity in males compared with females. Analysis of the three age-related groups demonstrated males having a higher global transitivity at all age ranges, with the high global modularity in the later years past the age of 13.1 y. This suggests that the preadolescent male brains are potentially beginning to reorganize and optimize certain subnetworks, displaying significant enhancement in modularity only in adolescence. Dense networks are thus observed in adolescence that continue to optimize into adulthood. On the contrary, females begin to develop higher long-range connectivity (mainly interhemispheric).

Our observations of increased participation coefficients in females is consistent with global measures of modularity, transitivity, *HCR*, and *LCW* (Table 2), all of which indicated increased intrahemispheric connectivity in males and interhemispheric connectivity in females. For example, lower modularity in females was corroborated by an increased regional participation coefficient (Fig. 3 and Table 3), which indicated that certain regions (frontal, temporal, and parietal lobes) had greater across-lobe connectivity in females; notably, this was mainly between lobes in different hemispheres as shown via the *HCR*. Conversely, the cerebellum, which exerts its influence on ipsilateral motor behavior through connectivity to contralateral supratentorial areas, was the only structure with the opposite pattern. This was confirmed
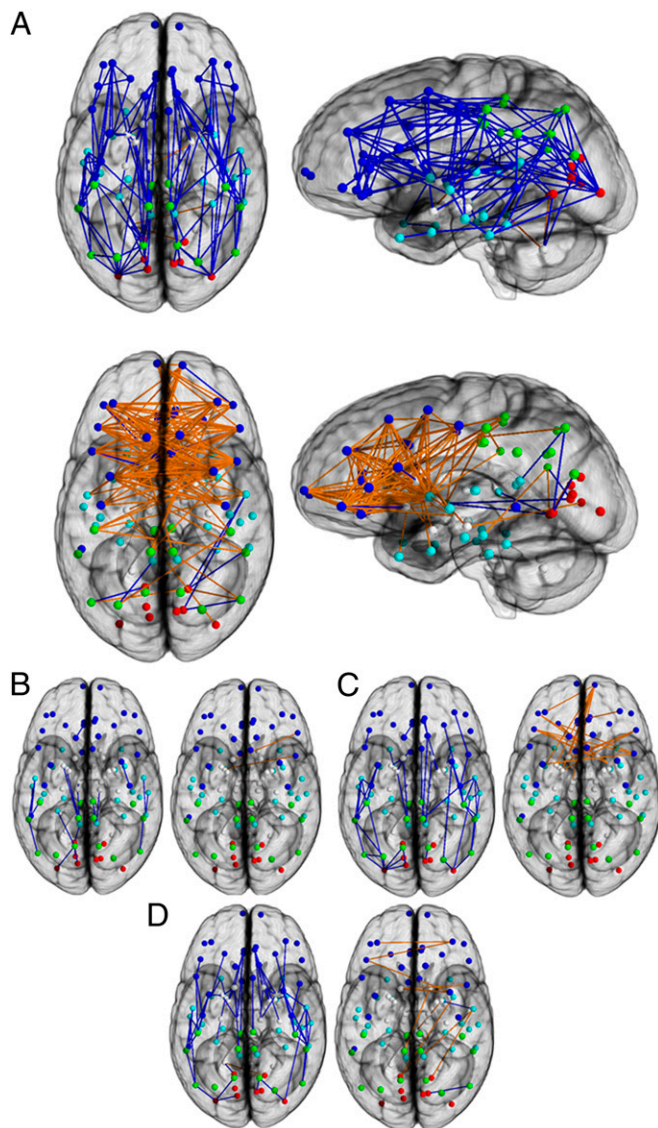
Fig. 2. Connection-wise analysis. (*A*) Brain networks show increased connectivity in males (*Upper*) and females (*Lower*). Analysis on the child (*B*), adolescent (*C*), and young adult (*D*) groups is shown. Intrahemispheric connections are shown in blue, and interhemispheric connections are shown in orange. The depicted edges are those that survived permutation testing at *P* = 0.05. Node color representations are as follows: light blue, frontal; cyan, temporal; green, parietal; red, occipital; white, subcortical. GM, gray matter.

via connection-based analysis (Fig. 2*A*), which showed the left cerebellum to be connected significantly to the lobes contralaterally in males, as well as through the participation coefficient of the cerebellum, which was significantly higher in males.

Taken together, these results reveal fundamental sex differences in the structural architecture of the human brain. Male brains during development are structured to facilitate within-lobe and within-hemisphere connectivity, with networks that are transitive, modular, and discrete, whereas female brains have greater interhemispheric connectivity and greater cross-hemispheric participation. Within-hemispheric cortical processing along the posterior-anterior dimension involves the linking of perception to action, and motor action is mediated ipsilaterally by the cerebellum. Greater within-hemispheric supratentorial connectivity combined with greater cross-hemispheric cerebellar connectivity would confer an efficient system for coordinated

Table 2. *LCW* differences between genders

Connection	*T* statistic	*P* value
LF-LF	5.06	<0.000001
LF-LT	5.06	<0.000001
LF-LP	7.29	<0.000001
LT-LT	7.15	<0.000001
LT-LP	5.07	<0.000001
LT-LO	5.95	0.000001
LP-LP	6.78	<0.000001
LP-LO	4.03	0.000061
LO-LO	4.89	<0.000001
LF-RF	−4.74	0.0000024
RF-RF	5.63	<0.000001
RF-RT	5.02	<0.000001
RF-RP	7.39	<0.000001
RT-RT	5.65	<0.000001
RT-RP	4.77	0.000002
RT-RO	5.26	<0.000001
RP-RP	5.83	<0.000001
RP-RO	3.22	0.00013
RO-RO	3.78	0.00017

A positive *T* statistic indicates that the male group had higher value than the female group, and vice versa. F, frontal; L, left; O, occipital; P, parietal; R, right; T, temporal.

action in males. Greater interhemispheric connectivity in females would facilitate integration of the analytical and sequential reasoning modes of the left hemisphere with the spatial, intuitive processing of information of the right hemisphere. A behavioral study on the entire sample, of which this imaging study is a subset, demonstrated pronounced sex differences, with the females outperforming males on attention, word and face memory, and social cognition tests and males performing better on spatial processing and motor and sensorimotor speed (2). These differences were mainly observed in midadolescent age (12–14 y), where males performed significantly faster on motor tasks and more accurately on spatial memory tasks. Other behavioral studies have found similar sex differences (41, 42). These behavioral studies are carried out at a denser age sampling, which is not possible for the imaging studies because the sample size in the subgroups will be too small to identify meaningful differences.

In addition to the consistency with the behavioral tasks, our findings on anatomical connectivity obtained with diffusion imaging are consistent with previous data from T1 structural imaging, showing a higher proportion of cortical WM in males (5), except for the CC (43). They are also consistent with activation studies using functional MRI, which have reported greater interhemispheric activation in females on a language task, in which they excelled (44), and greater focal intrahemispheric activation in males on a spatial task, in which they excelled (45). With respect to development, DTI studies (23, 24) have shown higher FA and lower MD in the CC in females during midadolescence, confirming a similar trend in our data. Although FA and MD provide measures of WM integrity, connectomic studies like ours are required to complete the picture of connection-wise systems.

Thus, the current study presents unique insights into sex differences using structural connectivity and measures defined on the connectome. Results are lent credence by supporting behavioral and functional studies. Our findings support the notion that the behavioral complementarity between the sexes has developmental neural substrates that could contribute toward improved understanding of this complementarity.

Materials and Methods

Dataset. Institutional Review Board approval was obtained from the University of Pennsylvania and the Children's Hospital of Philadelphia. The study includes 949 subjects (Table 1). For each subject, DTI [repetition time (TR)/echo time (TE) = 8,100/82 ms, resolution = 1.9 × 1.9 × 2 mm, 64 diffusion
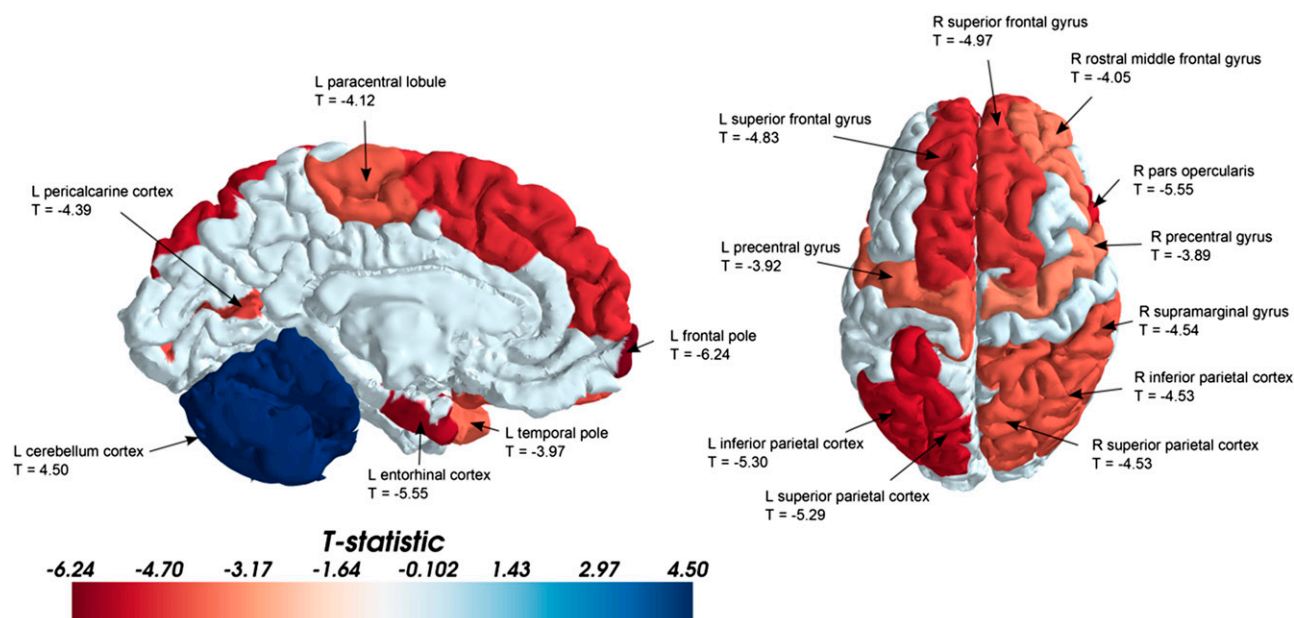
Ingalhalikar et al.

Fig. 3. Representative regions of the brain that have a higher *PC* at a significance level of *P* < 0.001. The regions have been projected onto the surface of the brain for better visualization. Red indicates a higher *PC* in the females, and blue indicates a higher *PC* in males (mainly localized to the cerebellum). Representative regions and their corresponding *T* values are shown in the figures. The other regions that show significant differences (with their respective *T* values; negative values indicate females > males) are listed in Table 3. These tests revealed that although multiple regions have higher *PCs* in females, the cerebellum has a higher *PC* in males. L, left; R, right.

directions with b = 1,000 s/mm^2 and 7 b = 0 images] and T1-weighted (TR/TE = 1,810/3.51 ms) MRI scans were acquired on the same Siemens 3T Verio scanner using a 32-channel head coil. Diffusion tensors were fitted to the DTI data (13–15), and FA maps were computed.

Creating SCs. The brain of each subject was parcellated into 95 regions of interest (ROIs; 68 cortical and 27 subcortical regions) of the Desikan atlas (46) using FreeSurfer (47) to act as node labels. The quality of the parcellation was manually checked for each subject. Each node label was treated as a seed region, and fibers were tracked probabilistically (48) from it to the other ROIs. We used the default parameters of two fibers per voxel and

Table 3. Sex differences in *PCs*

Node	T statistic	
	Left	Right
Frontal pole	−6.23711	−6.01209
Pars opercularis	−5.28418	−5.55390
Paracentral	−4.12355	
Superior frontal	−4.82684	−4.96510
Precentral	−3.91810	−3.89022
Supramarginal		−4.53635
Lateral orbitofrontal	−4.32909	
Inferior parietal	−5.30166	−4.52717
Rostral middle frontal		−4.05266
Superior parietal	−5.29189	−4.52765
Entorhinal	−5.54515	−4.65705
Bank of superior temporal sulcus	−5.11583	−6.70404
Pericalcarine	−4.39314	−3.62391
Temporal pole	−3.96837	
Caudate	−4.67867	−5.41545
Putamen	−3.88072	−5.51831
Pars triangularis	−3.91473	
Cerebellum	4.50010	3.69553

The *t* test on *PCs* revealed that many nodes have higher *PCs* in females than in males, except for the cerebellum, which has a higher *PC* in males.

5,000 sample streamlines for each tract to create a 95 × 95 matrix, *P*, of probability values. Each matrix entry P_{ij} represents a scaled conditional probability of a pathway between the seed ROI, *i*, and the target ROI, *j*, given by $P_{ij} = \frac{S_{i \rightarrow j}}{S_i} R_i$, where $S_{i \rightarrow j}$ denotes the number of fibers reaching the target region *j* from the seed region *i* and S_i is the number of streamlines seeded in *i*. We scale this ratio by the surface area R_i of the ROI, *i*, that accounts for different sizes of the seed region. This measure [like those found in previous studies (49–52)] quantifies connectivity such that $P_{ij} \approx P_{ji}$, which, on averaging, gives an undirected weighted connectivity measure. This now creates a 95 × 95 undirected symmetrical weighted connectivity network, *W*, called the SC. Fig. 1 gives a schematic for the pipeline.

Connectivity Analysis. In comparing general connectivity between groups (here, males and females), we look for significant connection-based difference in the SC *W*. Each connection weight P_{ij} was linearly regressed on age, sex, and age–sex interaction, and the resulting sex *T* statistic was used to construct the output *T* matrix (95 × 95). *T* was thresholded at positive and negative values to retain only those connections that are significantly stronger in either group. A positive T_{ij} indicates higher connectivity in the males, and a negative T_{ij} indicates higher connectivity in females.

We used a nonparametric method known as permutation testing, specifically a single-threshold test, to address the problem of multiple comparisons (53) on these high-dimensional network matrices (54). We randomized the labels (males/females) 20,000 times to create 20,000 *T* matrices and found the maximum *T* statistic of the entire network for each of the permutations to capture differences in the network. A histogram of these maximum *T* statistics over the entire network for each permutation was then constructed, and a threshold value was computed at a significance level of 0.05. Finally, this threshold was applied on the regression statistics performed on age, sex, and age–sex interaction. The connections with a higher *T* statistic value than the threshold were the ones that survived the correction. The three groups (children, adolescents, and young adults) were tested in a similar manner, again at *P* = 0.05 and with 10,000 permutations.

Network Measures. The structural network was analyzed at several levels of granularity, from connection-based measures as described above to measures of modularity and transitivity at macroscopic, lobar, and regional levels. *HCR.* This quantifies the dominance of intra- or interhemispheric connections in the network matrices. It is the ratio of a lobe's number of intrahemispheric connections to its number of interhemispheric connections.

LCW. To assess both intra- and interlobe connectivity, we define an *LCW* for each pair of lobes (L_x, L_y): $LCW(L_x, L_y) = \sum_{i \in L_x, j \in L_y} w_{ij}$, where w_{ij} is the connectivity weight between regions i and j. For each *LCW* (L_x, L_y), a *T* statistic was computed between males and females while covarying for age and race. **Modularity.** Modularity reflects how well the network can be delineated into groups (or communities), as defined via spectral clustering that maximizes the number of intragroup connections and minimizes the number of intergroup connections. A modularity measure is then calculated from the community structure based on the proportion of links connecting regions in different groups. The weighted modularity of a network is defined as follows: $M = \frac{1}{T} \sum_{i,j \in N} \left[w_{ij} - \frac{k_i k_j}{z} \right]$, where w_{ij} is the connectivity weight between the regions i and j, k_i is the sum of the connection weights of i, and z is the sum of all connection weights in the network.
Transitivity. The transitivity of a network or subnetwork, $T = \frac{\sum_{i \in N} 2 t_i}{\sum_{i \in N} k_i(k_i - 1)}$, where t_i is the weighted geometric mean of the triad of regions around the region I, quantifies the proportion of fully connected triads of regions whose neighbors are also immediate neighbors of each other, with high transitivity indicating increased local connectivity. Transitivity is also calculated

by considering lobes as subnetworks, where the brain is divided into eight lobes: right and left temporal, right and left frontal, right and left parietal, and right and left occipital. Eight anatomically consistent lobe networks are constructed from the resulting submatrices of these.
PC. This is a regional measure that compares the total weight of the region's intralobar connections against the total weight of its interlobar connections.

The PC of a region y_i is given by $PC(y_i) = 1 - \sum_{m \in M} \left(\frac{k_i(m)}{k_i} \right)^2$, where M is the set of subnetworks (lobes in our case) and $k_i(m)$ is the sum of the weights of all connections between i and regions in subnetwork m. A low PC indicates reduced connectivity to other subnetworks and/or increased connectivity within its own subnetwork.

1. Jazin E, Cahill L (2010) Sex differences in molecular neuroscience: From fruit flies to humans. *Nat Rev Neurosci* 11(1):9–17.
2. Gur RC, et al. (2012) Age group and sex differences in performance on a computerized neurocognitive battery in children age 8-21. *Neuropsychology* 26(2):251–265.
3. Halpern D (2007) The science of sex differences in science and mathematics. *Psychol Sci Public Interest* 8(1):1–51.
4. Allen JS, Damasio H, Grabowski TJ, Bruss J, Zhang W (2003) Sexual dimorphism and asymmetries in the gray-white composition of the human cerebrum. *Neuroimage* 18(4):880–894.
5. Gur RC, et al. (1999) Sex differences in brain gray and white matter in healthy young adults: Correlations with cognitive performance. *J Neurosci* 19(10):4065–4072.
6. Goldstein JM, et al. (2001) Normal sexual dimorphism of the adult human brain assessed by in vivo magnetic resonance imaging. *Cereb Cortex* 11(6):490–497.
7. Cosgrove KP, Mazure CM, Staley JK (2007) Evolving knowledge of sex differences in brain structure, function, and chemistry. *Biol Psychiatry* 62(8):847–855.
8. Giedd JN, et al. (1996) Quantitative MRI of the temporal lobe, amygdala, and hippocampus in normal human development: Ages 4-18 years. *J Comp Neurol* 366(2):223–230.
9. Giedd JN, Castellanos FX, Rajapakse JC, Vaituzis AC, Rapoport JL (1997) Sexual dimorphism of the developing human brain. *Prog Neuropsychopharmacol Biol Psychiatry* 21(8):1185–1201.
10. Allen LS, Richey MF, Chai YM, Gorski RA (1991) Sex differences in the corpus callosum of the living human being. *J Neurosci* 11(4):933–942.
11. Courchesne E, et al. (2000) Normal brain development and aging: Quantitative analysis at in vivo MR imaging in healthy volunteers. *Radiology* 216(3):672–682.
12. Coffey CE, et al. (1998) Sex differences in brain aging: A quantitative magnetic resonance imaging study. *Arch Neurol* 55(2):169–179.
13. Basser PJ, Jones DK (2002) Diffusion-tensor MRI: Theory, experimental design and data analysis—A technical review. *NMR Biomed* 15(7-8):456–467.
14. Basser PJ, Mattiello J, LeBihan D (1994) MR diffusion tensor spectroscopy and imaging. *Biophys J* 66(1):259–267.
15. Le Bihan D, et al. (2001) Diffusion tensor imaging: Concepts and applications. *J Magn Reson Imaging* 13(4):534–546.
16. Pierpaoli C, Basser PJ (1996) Toward a quantitative assessment of diffusion anisotropy. *Magn Reson Med* 36(6):893–906.
17. Herting MM, Maxwell EC, Irvine C, Nagel BJ (2012) The impact of sex, puberty, and hormones on white matter microstructure in adolescents. *Cereb Cortex* 22(9):1979–1992.
18. Westerhausen R, et al. (2003) The influence of handedness and gender on the microstructure of the human corpus callosum: A diffusion-tensor magnetic resonance imaging study. *Neurosci Lett* 351(2):99–102.
19. Hsu JL, et al. (2008) Gender differences and age-related white matter changes of the human brain: A diffusion tensor imaging study. *Neuroimage* 39(2):566–577.
20. Kanaan RA, et al. (2012) Gender differences in white matter microstructure. *PLoS ONE* 7(6):e38272.
21. Schmithorst VJ, Holland SK, Dardzinski BJ (2008) Developmental differences in white matter architecture between boys and girls. *Hum Brain Mapp* 29(6):696–710.
22. Kumar R, Nguyen HD, Macey PM, Woo MA, Harper RM (2012) Regional brain axial and radial diffusivity changes during development. *J Neurosci Res* 90(2):346–355.
23. Bava S, et al. (2011) Sex differences in adolescent white matter architecture. *Brain Res* 1375:41–48.
24. Asato MR, Terwilliger R, Woo J, Luna B (2010) White matter development in adolescence: A DTI study. *Cereb Cortex* 20(9):2122–2131.
25. Abe O, et al. (2010) Sex dimorphism in gray/white matter volume and diffusion tensor during normal aging. *NMR Biomed* 23(5):446–458.
26. Lebel C, Caverhill-Godkewitsch S, Beaulieu C (2010) Age-related regional variations of the corpus callosum identified by diffusion tensor tractography. *Neuroimage* 52(1):20–31.
27. Eluvathingal TJ, Hasan KM, Kramer L, Fletcher JM, Ewing-Cobbs L (2007) Quantitative diffusion tensor tractography of association and projection fibers in normally developing children and adolescents. *Cereb Cortex* 17(12):2760–2768.
28. Clayden JD, et al. (2012) Normative development of white matter tracts: Similarities and differences in relation to age, gender, and intelligence. *Cereb Cortex* 22(8):1738–1747.
29. Sporns O (2011) The human connectome: A complex network. *Ann N Y Acad Sci* 1224:109–125.
30. Bullmore E, Sporns O (2009) Complex brain networks: Graph theoretical analysis of structural and functional systems. *Nat Rev Neurosci* 10(3):186–198.
31. Hagmann P, et al. (2008) Mapping the structural core of human cerebral cortex. *PLoS Biol* 6(7):e159.
32. Tomasi D, Volkow ND (2012) Laterality patterns of brain functional connectivity: Gender effects. *Cereb Cortex* 22(6):1455–1462.
33. Tomasi D, Volkow ND (2012) Gender differences in brain functional connectivity density. *Hum Brain Mapp* 33(4):849–860.
34. Iturria-Medina Y, et al. (2007) Characterizing brain anatomical connections using diffusion weighted MRI and graph theory. *Neuroimage* 36(3):645–660.
35. Iturria-Medina Y, Sotero RC, Canales-Rodríguez EJ, Alemán-Gómez Y, Melie-García L (2008) Studying the human brain anatomical network via diffusion-weighted MRI and Graph Theory. *Neuroimage* 40(3):1064–1076.
36. Yan C, et al. (2011) Sex- and brain size-related small-world structural cortical networks in young adults: A DTI tractography study. *Cereb Cortex* 21(2):449–458.
37. Gong G, et al. (2009) Age- and gender-related differences in the cortical anatomical network. *J Neurosci* 29(50):15684–15693.
38. Dennis EL, et al. (2013) Development of brain structural connectivity between ages 12 and 30: A 4-Tesla diffusion imaging study in 439 adolescents and adults. *Neuroimage* 64:671–684.
39. Rubinov M, Sporns O (2010) Complex network measures of brain connectivity: Uses and interpretations. *Neuroimage* 52(3):1059–1069.
40. Steinmetz H, Staiger JF, Schlaug G, Huang Y, Jäncke L (1995) Corpus callosum and brain volume in women and men. *Neuroreport* 6(7):1002–1004.
41. Cherney ID, Brabec CM, Runco DV (2008) Mapping out spatial ability: Sex differences in way-finding navigation. *Percept Mot Skills* 107(3):747–760.
42. Hamilton C (2008) *Cognition and Sex Differences* (Palgrave Macmillan).
43. Dubb A, Gur R, Avants B, Gee J (2003) Characterization of sexual dimorphism in the human corpus callosum. *Neuroimage* 20(1):512–519.
44. Shaywitz BA, et al. (1995) Sex differences in the functional organization of the brain for language. *Nature* 373(6515):607–609.
45. Gur RC, et al. (2000) An fMRI study of sex differences in regional activation to a verbal and a spatial task. *Brain Lang* 74(2):157–170.
46. Desikan RS, et al. (2006) An automated labeling system for subdividing the human cerebral cortex on MRI scans into gyral based regions of interest. *Neuroimage* 31(3):968–980.
47. Fischl B, Sereno MI, Dale AM (1999) Cortical surface-based analysis. II: Inflation, flattening, and a surface-based coordinate system. *Neuroimage* 9(2):195–207.
48. Behrens TE, et al. (2003) Characterization and propagation of uncertainty in diffusion-weighted MR imaging. *Magn Reson Med* 50(5):1077–1088.
49. Hagmann P, et al. (2010) White matter maturation reshapes structural connectivity in the late developing human brain. *Proc Natl Acad Sci USA* 107(44):19067–19072.
50. Bassett DS, et al. (2008) Hierarchical organization of human cortical networks in health and schizophrenia. *J Neurosci* 28(37):9239–9248.
51. Gong G, et al. (2009) Mapping anatomical connectivity patterns of human cerebral cortex using in vivo diffusion tensor imaging tractography. *Cereb Cortex* 19(3):524–536.
52. Sporns O, Honey CJ, Kötter R (2007) Identification and classification of hubs in brain networks. *PLoS ONE* 2(10):e1049.
53. Holmes AP, Blair RC, Watson JD, Ford I (1996) Nonparametric analysis of statistic images from functional mapping experiments. *J Cereb Blood Flow Metab* 16(1):7–22.
54. Nichols TE, Holmes AP (2002) Nonparametric permutation tests for functional neuroimaging: A primer with examples. *Hum Brain Mapp* 15(1):1–25.

Ingalhalikar et al.